IEEE Access
Multidisciplinary | Rapid Review | Open Access Journal

Received November 27, 2018, accepted January 9, 2019, date of publication January 14, 2019, date of current version February 6, 2019.

Digital Object Identifier 10.1109/ACCESS.2019.2892822

Multivector Sparse Representation for Multispectral Images Using Geometric Algebra

RUI WANG[1], (Member, IEEE), MIAOMIAO SHEN[1], AND WENMING CAO[2], (Member, IEEE)
[1]Communication and Information Engineering, Shanghai University, Shanghai 200444, China
[2]College of Information Engineering, Shenzhen University, Shenzhen, China

Corresponding author: Wenming Cao (wmcao@szu.edu.cn)

This work was supported by the National Natural Science Foundation of China under Grant 61771299, Grant 61771322, Grant 61375015, and Grant 61301027.

ABSTRACT Multispectral images can provide more faithful representations for real scenes than the traditional images and improve the performance of image restoration tasks. In this paper, we propose a novel multivector sparse representation model for multispectral images using geometric algebra (GA), with the truth that GA is now well used in image processing and it gives a formidable way to represent multispectral images. The proposed model represents a multispectral image as a GA multivector by fully considering the spatial and spectral information, where a GA dictionary learning algorithm is presented using the K-GA-singular value decomposition (GASVD) (generalized K-means clustering for GASVD) method. Consequently, with the complete consideration of the relationship between spectral channels in multispectral images, artifacts and blurring effects can be successfully avoided. The experimental results demonstrate that the proposed sparse model surpasses the existing methods for multispectral images reconstruction and denoising tasks by capturing correlations between spectral channels thoroughly and shows its usefulness and effectiveness for multispectral images processing.

INDEX TERMS Multivector, sparse representation, geometric algebra (GA), multispectral images, dictionary learning, K-GASVD.

I. INTRODUCTION

Recently, multispectral images have been widely applied in more and more areas, e.g., medical image analysis, military defense, environmental monitoring, space remote sensing, geological exploration, digital photography, etc. [1]–[3], due to the large amount of information it contains. Combined with spatial and spectral information, multispectral images specifically consist of visible light, infrared ray, ultraviolet radiation, millimeter wave or X-ray. That is to say, a multispectral image is formed with multiple scalar images, in which each image is usually regarded as a band or a channel, at specific frequencies across the electromagnetic spectrum. Substantially, the performance of multiple computer vision tasks, such as tracking, and inpainting [4], [5], have been dramatically enhanced due to such comprehensive knowledge representation capability of multispectral images. Therefore, the processing techniques for multispectral images have become quite emerging topics, which bring both opportunities and challenges [6]–[8].

In image processing and analysis domain, sparse representation [9], [10] has occupied an important place, and has witnessed great success in variety of tasks, e.g., natural image denoising [11], [12], reconstruction [12], classification [13], [14], detection [15], and restoration [16]. The K-SVD algorithm [11] was utilized to show great performance in a wide range of gray-scale image processing, but it leaded to some unsatisfying results for color image due to the loss of relationship between RGB channels. Mairal *et al.* [16] provided a simple concatenation of the RGB values of a color image to a single vector and training on those directly, which gives already better results than performing each channel separately. However, such a process produces false colors and artifacts. Xu *et al.* [18] provided an efficient color sparse representation model on account of the compatibility between quaternion matrix and color image to avoid losing the correlation of three color channels. Wang *et al.* [19] applied geometric algebra to map the color image into a high-dimensional space to color image analysis

and achieved high performance. To address the problem of high computational complexity owing to non-commutative multiplication, Shen *et al.* [20] presented a novel theory of reduced geometric algebra (RGA) with commutative multiplication rules and a novel vector-valued sparse representation model for color image using RGA. Shen and Wang [21] then proposed a new singular value decomposition algorithm for octonion signals, which can be simply regarded as seven-channel multispectral images. However, existing sparse models are mostly developed for gray or 3-channel color images [17], [18], [22], and there are very few works focusing on the sparse representation of multichannel signals, typically as multispectral images.

Fortunately, geometric algebra (GA) provides a powerful computing framework in signal and image processing and it gives a formidable way for multi-dimensional signals [23]–[25]. Ebling and Scheuermann [26] extended the Fourier transform to (multi)vector fields using GA and verify the generalizations of correlation, convolution and derivative theorems. Wang *et al.* [27] created a sparse fast Clifford Fourier transform based on GA, which showed great improvement in computing performance over scalar and vector fields. Li *et al.* [28] put forward a new SIFT algorithmic framework based on GA for multispectral images processing and analysis.

Inspired by the useful information contained in multispectral images, the recent progress of sparse representation models and the advantages of GA theory in various fields of image processing, we present a novel multivector sparse representation model, which adopts GA framework to leverage the multispectral information. Due to the utilization of the GA theory, both spatial and spectral information of multispectral images can be completely retained, and the inherent spectral structures in multispectral images can be preserved successfully during sparse reconstruction without losing the relationship of spectral channels. Besides, in terms of training process, we correspondingly design the dictionary learning algorithm based on GA, namely K-GASVD (K-means clustering for singular value decomposition based on GA) to obtain a trained dictionary that contains the richest spectral information. In summary, the GA dictionary converts the channel images to a subspace in a uniform way, and consequently the inherent spectral structures can be successfully preserved during vector reconstruction.

The major contribution of this paper lies in the following aspects. Firstly, a multispectral image is successfully represented as a GA multivector, in which each spectral channel is mapped to each blade of GA. Secondly, we propose a novel and efficient multivector sparse representation model based on GA on account of the compatibility between a GA multivector and a multispectral image to avoid losing the correlation of spectral channels. Thirdly, we develop an effective dictionary learning method based on GA, namely K-GASVD, which has the ability to update coefficient simultaneously instead of fixing the coefficient vector during dictionary learning. Extensive experiments of multispectral images reconstruction and denoising indicate that superior performance is achieved with the proposed sparse model.

The remainder of this paper is organized as follows. Section II reviews the existing sparse models and basis of geometric algebra (GA) briefly. The proposed sparse model for multispectral images is illustrated in Section III. GA-based SVD and dictionary training methods are described in Section IV. Reconstruction and denoising experiments for multispectral images using our proposed model are presented in Section V, and the conclusion of this paper is given in Section VI.

II. RELATED WORK

A. REVIEW OF CURRENT SPARSE REPRESENTA-TION MODELS

As a powerful and vibrant method to represent images utilizing redundant dictionaries, image sparse representations that mostly focused on patch processing, have enjoyed great popularity as a means for image processing and analysis. It is well known that existing sparse models have been very successful in handling single channel gray-scale images as well as 3-channel color images, in which every color channel is associated with each other.

Sparse model based on K-SVD method [11] has achieved great performance in gray-scale image domain, and can be formulated by

$$min_{a_s} \|a_s\|_0 , \quad s.t. f_s = D_s a_s \tag{1}$$

where $f_s \in \mathbb{R}^n$ is the gray-scale image patch, $D_s \in \mathbb{R}^{n\times m}$ is the corresponding dictionary, and $a_s \in \mathbb{R}^m$ is the assumed sparse coefficient vector. Nevertheless, for color image, it just regards RGB channels as three independent ''gray-scale'' images and processes them in a monochrome way, which loses the inter-correlation among the three-color channels leading to some unsatisfying results.

To further avoid the loss of relationship among channels in a color image, the approach put forward in [16] concatenated the three channels into a single channel to train a common dictionary and share a common coefficient vector, the concatenation model is described as follows

$$\begin{bmatrix} y_r^T & y_g^T & y_b^T \end{bmatrix}^T = \begin{bmatrix} D_r^T & D_g^T & D_b^T \end{bmatrix}^T a \tag{2}$$

Though, the concatenation model in (2) partly addressed the loss of inherent color structure compared to (1), it inevitably produced some unsatisfying results such as false colors and artifacts.

When dealing with color image, the most urgent problem needed to be addressed is to avoid the loss of inherent relationship of RGB channels. Wang *et al.* [19] applied geometric algebra to denote the structure of color information and map the color image into a high-dimensional space, and the model has been, until very recently, regarded as a powerful model for color image processing. Each color image patch can be represented as $f = 0 + f_1 e_1 + f_2 e_2 + f_{12} e_{12} \in (\mathbb{G}_2)^N$ while applying GA, and the sparse representation model in $\mathbb{G}_2$ has

been given as

$$min_g \|g\|_0, \quad s.t. f = Dg \tag{3}$$

where $D = 0 + D_1e_1 + D_2e_2 + D_{12}e_{12} \in (\mathbb{G}_2)^{N\times M}$ is a dictionary in $\mathbb{G}_2$, $g = 0 + g_1e_1 + g_2e_2 + g_{12}e_{12} \in (\mathbb{G}_2)^M$ is a corresponding sparse coefficient vector, with its components g_1, g_2 and $g_{12} \in \mathbb{R}^M$. Here, $\mathbb{G}_2$ denotes the 2-dimensional GA space.

Compared with the K-SVD based sparse model in (1), the sparse representation model in $\mathbb{G}_2$ deals with three color channels information in a unified way to imitate the process of human visual perception. The coefficient matrix captures both the relationship of color channels and the orthogonal property successfully. The obvious advantage is that it maintains the inherent structures of RGB channels during image reconstruction.

In retrospect, the performance improvements of these recent attempts have been ascribed to their use of algebraic frameworks and, until now, very few researches have been conducted in handling high dimensional data, typically as multispectral images. Then, in this paper, we pay more attention to retain the correlation of each spectral channel by representing the multispectral images and subsequently propose a multivector sparse representation model based on geometric algebra.

B. REPRESENTATION MODELS FOR MULTISPECTRAL IMAGES

Since multispectral images have recently attracted much attention and there have emerged many representation methods. Huang *et al.* [29] presented a novel spatial and spectral fusion model (SASFM) that uses sparse matrix factorization to fuse remote sensing imagery with different spatial and spectral properties. Lanaras *et al.* [30] jointly processed high spectral and high geometric resolution images and exploited their synergies to generate a fused image of high spectral and geometric resolution, and improve (linear) spectral unmixing of hyperspectral endmembers at subpixel level, which is the pixel size of the hyperspectral image. Dian *et al.* [31] proposed a novel hyperspectral image (HIS) super-resolution method based on non-local sparse tensor factorization (called as the NLSTF). The sparse tensor factorization can directly decompose each cube of the HSI as a sparse core tensor and dictionaries of three modes, which reformulates the HSI super-resolution problem as the estimation of sparse core tensor and dictionaries for each cube. Zhang *et al.* [32] proposed a new low-resolution HS (LRHS) and high-resolution MS (HRMS) image fusion method based on spatial-spectral-graph-regularized low-rank tensor decomposition (SSGLRTD) to effectively preserve spatial-spectral structures in HRHS images.

C. THE BASICS OF GEOMETRIC ALGEBRA

William K. Clifford introduced Geometric Algebra abbreviated as GA, also called Clifford Algebra, which provides such a coordinate-free framework to make the computation efficiently [23]–[25]. It completes the constructions and modelings in a coordinate-free way and also has revealed wide applications especially when applying to computer vision tasks [26]–[28].

Suppose $\mathbb{G}_n$ is n -dimensional GA with an orthonormal basis of vectors $\{e_i\}, i = 1, \cdots, n$, which leads to a basis

$$\left\{1, \{e_i\}, \{e_ie_j\}, \cdots, \{e_1e_2\cdots e_n\}\right\} \tag{4}$$

Specifically, $\mathbb{G}_n$ can be represented by $\mathbb{G}_{p,q}$, where $n = p + q$ and p, q are the number of vectors with positive square and negative square in the basis of the space, respectively. That is

$$e_i^2 = \begin{cases} 1, & 1 \leqslant i \leqslant p \\ -1, & p+1 \leqslant i \leqslant n \end{cases} \tag{5}$$

In this paper, we focus on $\mathbb{G}_n$, in which $q = 0$. Generally, the geometric product of two basis is anti-commutative, and

$$e_ie_j = e_{ij} = -e_je_i = -e_{ji}, \quad i, j = 1, \cdots, n, i \neq j \tag{6}$$

$$e_i^2 = 1, \quad i = 1, \cdots, n \tag{7}$$

$$e_ie_{ij} = e_ie_ie_j = e_j, \quad i, j = 1, \cdots, n, i \neq j \tag{8}$$

Given two vectors w and z in $\mathbb{G}_n$, the geometric product is given by

$$wz = w \cdot z + w \wedge z \tag{9}$$

where $w \cdot z$ denotes the inner product and $w \wedge z$ is the outer product. Since the vectors are orthogonal, then $e_ie_j = e_i \cdot e_j + e_i \wedge e_j = e_i \wedge e_j$.

Take $\mathbb{G}_3$ for instance, the orthogonal bases are constructed by vectors with $2^3 = 8$ grades, which is given by: $\left\{1, \{e_1, e_2, e_3\}, \{e_1e_2, e_1e_3, e_2e_3\}, \{e_1e_2e_3\}\right\}$ and a simpler form: $\{1, e_1, e_2, e_3, e_{12}, e_{13}, e_{23}, e_{123}\}$. For a 2^n -dimensional signal, only basis is needed. Generally, the outer product of k vectors is called a k-blade. The number k is called the grade of the blade.

In GA space, multivectors, which stand for the extension of vectors in higher dimensions, are the basic elements. Any multivector $M \in \mathbb{G}_n$ is described by

$$M = E_0 + \sum_{1\leqslant i\leqslant n} E_i(M)e_i + \sum_{1\leqslant i<j\leqslant n} E_{ij}(M)e_{ij} + \cdots + E_{1\cdots n}(M)e_{1\cdots n} \tag{10}$$

where $E(M) \in \mathbb{R}$.

III. THE MULTIVECTOR SPARSE REPRESENTATION MODEL FOR MULTISPECTRAL IMAGES

In this section, we utilize geometric algebra (GA) to extend the sparse model in (3) for color image to multispectral images.

A. REPRESENTATION OF MULTISPECTRAL IMAGES USING GA

Each pixel of a multispectral image I can be denoted in $\mathbb{G}_n$ as follows.

$$I(x,y) = 0 + \sum_{1\leqslant i\leqslant n} I_i(x,y)e_i + \sum_{1\leqslant i<j\leqslant n} I_{ij}(x,y)e_{ij} + \cdots + I_{1\cdots n}(x,y)e_{1\cdots n} \quad (11)$$

where $I_i(x,y), I_{ij}(x,y), I_{1\cdots n}(x,y)$ are the spectral components of multispectral image pixel $I(x,y)$ at position (x,y) respectively.

Specifically, all the spectral channels of the multispectral image are assigned to the basis

$$\left\{1, \left\{e_i\right\}, \left\{e_i e_j\right\}, \cdots, \left\{e_1 e_2 \cdots e_n\right\}\right\}$$

of the 2^n -dimensional GA $(\mathbb{G}_n)$ respectively, and a GA multivector is used to rewrite the multispectral images pixel $I(x,y)$ in GA space.

Thus, a multispectral image $F \in (\mathbb{G}_n)^{M\times N}$ with M rows and N columns can be represented by a GA multivector

$$F = 0 + \sum_{1\leqslant i\leqslant n} E_i(F)e_i + \sum_{1\leqslant i<j\leqslant n} E_{ij}(F)e_{ij} + \cdots + E_{1\cdots n}(F)e_{1\cdots n}, E(F) \in \mathbb{R}^{M\times N} \quad (12)$$

Recently, the GA representation of multispectral images have attracted great attention. Since our work is not the first one to represent multispectral images using GA, the representation method based on GA introduced in this paper has some differences from the paper by Li *et al.* [28]. In the paper by Li *et al.*, it only uses 1-blade to represent a multispectral image (see [28, eq. (14)]) and ignores all the outer product parts (it says "There are two multivector in the result of the Eq. (27), and the second multivector cannot be used in the image processing simply."). In our paper, we reserve all the outer product parts, which brings the relationship of components in GA space into correspondence with the correlation of spectral channels in a multispectral image, and can be considered as a better and more comprehensive representation of a multispectral image. It can be applied in studying the problems of multispectral images processing due to its capability to treat the spectral channels holistically without losing the relationship of the spectral channels.

B. GA-MULTIVECTOR SPARSE REPRESENTATION MODEL FOR MULTISPECTRAL IMAGES

To take the correlation of the multispectral channels into consideration, we put forward a novel multivector sparse representation model using geometric algebra for multispectral images in this paper. For each patch $f \in (\mathbb{G}_n)^{\sqrt{N}\times\sqrt{N}}$ of the multispectral image $F \in (\mathbb{G}_n)^{N\times K}$, where N is the size of the multispectral image and K denotes the number of image patches. Then we transfer it to a vector $f \in (\mathbb{G}_n)^N$ with the length of N as follows

$$f = 0 + \sum_{1\leqslant i\leqslant n} E_i(f)e_i + \sum_{1\leqslant i<j\leqslant n} E_{ij}(f)e_{ij} + \cdots + E_{1\cdots n}(f)e_{1\cdots n}, E(f) \in \mathbb{R}^N \quad (13)$$

Then, we define our proposed multivector sparse representation model as follows

$$min_a \|a\|_0, \quad s.t.\, f = Da \quad (14)$$

where $D = \begin{pmatrix} E_0(D) + \sum_{1\leqslant i\leqslant n} E_i(D)e_i + \sum_{1\leqslant i<j\leqslant n} E_{ij}(D)e_{ij} \\ + \cdots + E_{1\cdots n}(D)e_{1\cdots n} \in (\mathbb{G}_n)^{N\times M} \end{pmatrix}$ is a GA dictionary consisting of M atoms and $E(D) \in \mathbb{R}^{N\times M}$. $a = \begin{pmatrix} E_0(a) + \sum_{1\leqslant i\leqslant n} E_i(a)e_i + \sum_{1\leqslant i<j\leqslant n} E_{ij}(a)e_{ij} \\ + \cdots + E_{1\cdots n}(a)e_{1\cdots n} \in (\mathbb{G}_n)^M \end{pmatrix}$ is a GA coefficient vector and $E(a) \in \mathbb{R}^M$. The objective function $\|a\|_0$ is resolved to collect all the number of non-zero components in the coefficient vector above.

The generalized form of representation model for multispectral images is derived in the Appendix A.

Specially, for a multispectral image $F' \in (\mathbb{G}_2)^{N\times K}$ with 3 channels, which can be represented in $\mathbb{G}_2$ space, and each patch $f' \in (\mathbb{G}_2)^{\sqrt{N}\times\sqrt{N}}$ can be transferred to a vector $f' \in (\mathbb{G}_2)^N$ with the length of N as follows

$$f' = 0 + E_1(f')e_1 + E_2(f')e_2 + E_{12}(f')e_{12} \in (\mathbb{G}_2)^N \quad (15)$$

Then, the proposed model in $\mathbb{G}_2$ space for 3 channels color image is defined as follows

$$min_{a'} \left\|a'\right\|_0, \quad s.t.\, f' = D'a' \quad (16)$$

where $D' = E_0(D') + E_1(D')e_1 + E_2(D')e_2 + E_{12}(D')e_{12}, D' \in (\mathbb{G}_2)^{N\times M}$ is defined as a GA dictionary with M atoms and a GA coefficient vector is shown as $a' = E_0(a') + E_1(a')e_1 + E_2(a')e_2 + E_{12}(a')e_{12}$.

Similarly, $\left\|a'\right\|_0$ is utilized to count the number of all the non-zero components in GA coefficient vector.

The generalized form of 3 channels color image sparse model can then be obtained as follows

$$\begin{bmatrix} 0 & E_1(f') & E_2(f') & E_{12}(f') \end{bmatrix} = \begin{bmatrix} E_0(D') & E_1(D') & E_2(D') & E_{12}(D') \end{bmatrix}(a') \quad (17)$$

Since

$$\begin{aligned} f' = D'a' &\Leftrightarrow 0 + E_1(f')e_1 + E_2(f')e_2 + E_{12}(f')e_{12} \\ &= \left(E_0(D') + E_1(D')e_1 + E_2(D')e_2 + E_{12}(D')e_{12}\right) \\ &\quad \times \left(E_0(a') + E_1(a')e_1 + E_2(a')e_2 + E_{12}(a')e_{12}\right) \\ &= \begin{pmatrix} E_0(D')E_0(a') + E_1(D')E_1(a') \\ E_2(D')E_2(a') - E_{12}(D')E_{12}(a') \end{pmatrix} \\ &\quad + \begin{pmatrix} E_0(D')E_1(a') + E_1(D')E_0(a') \\ -E_2(D')E_{12}(a') + E_{12}(D')E_2(a') \end{pmatrix} e_1 \\ &\quad + \begin{pmatrix} E_0(D')E_2(a') + E_1(D')E_{12}(a') \\ +E_2(D')E_0(a') - E_{12}(D')E_1(a') \end{pmatrix} e_2 \\ &\quad + \begin{pmatrix} E_0(D')E_{12}(a') + E_1(D')E_2(a') \\ -E_2(D')E_1(a') + E_{12}(D')E_0(a') \end{pmatrix} e_{12} \end{aligned} \quad (18)$$

Therefore, we can obtain

$$(a') = \begin{bmatrix} E_0(a') & E_1(a') & E_2(a') & -E_{12}(a') \\ E_1(a') & E_0(a') & -E_{12}(a') & E_2(a') \\ E_2(a') & E_{12}(a') & E_0(a') & -E_1(a') \\ E_{12}(a') & E_2(a') & -E_1(a') & E_0(a') \end{bmatrix} \quad (19)$$

IV. GA-BASED DICTIONARY TRAINING

In this section, we extend the singular value decomposition (SVD) to n-dimensional space using GA, and present the dictionary-learning problems.

A. GASVD ALGORITHM FOR MULTISPECTRAL IMAGES

Similar to the SVD of real data [33]–[35], for a GA multivector $F \in (\mathbb{G}_n)^{M\times N}$ of a multispectral image, then there exist two GA unitary matrix $U \in (\mathbb{G}_n)^{M\times M}$ and $V \in (\mathbb{G}_n)^{N\times N}$ such that

$$U^H F V = \begin{bmatrix} \Sigma' & 0 \\ 0 & 0 \end{bmatrix} \equiv \Sigma \in \mathbb{R}^{M\times N} \quad (20)$$

where $\Sigma' = diag\{\sigma_1, \sigma_2, \ldots, \sigma_P\} \in \mathbb{R}^{P\times P}$, σ_i are the positive singular values of F, $\sigma_1 \geq \sigma_2 \geq \cdots \geq \sigma_P$ and $P = min\{M, N\}$ and H represents the conjugate transpose operation.

That is, for any $M \times N$ GA multivector F, its SVD is obtained by

$$F = U\Sigma V^H = U \begin{bmatrix} \Sigma' & 0 \\ 0 & 0 \end{bmatrix} V^H \quad (21)$$

where $UU^H = \mathbb{I}^{M\times M}$, $VV^H = \mathbb{I}^{N\times N}$, $\mathbb{I}$ is an identity matrix.

We can perform the GA-SVD with different kinds of algorithms.

Suppose

$$F = \begin{pmatrix} E_0(F) + \sum_{1\leqslant i\leqslant n} E_i(F)e_i + \sum_{1\leqslant i<j\leqslant n} E_{ij}(F)e_{ij} \\ + \cdots + E_{1\cdots n}(F)e_{1\cdots n} \in (\mathbb{G}_n)^{M\times N} \end{pmatrix}$$

where $E(F) \in \mathbb{R}^{M\times N}$, its real representation F_R can be defined as (22), shown at the bottom of the next page.

Then using the isomorphism between $(\mathbb{G}_n)^{M\times N}$ and $\mathbb{R}^{2^n M\times 2^n N}$, the GASVD of F can be performed by employing the conventional real SVD algorithm to F_R. We define the relationship between the GASVD of a GA multivector F and the SVD of its equivalent real matrix F_R as follows

1) $\Sigma' = row_{odd}^{2^{n-1}}(col_{odd}^{2^{n-1}}(\Sigma'_R))$.

2) $U = \begin{pmatrix} E_0(U) + \sum_{1\leqslant i\leqslant n} E_i(U)e_i + \sum_{1\leqslant i<j\leqslant n} E_{ij}(U)e_{ij} \\ + \cdots + E_{1\cdots n}(U)e_{1\cdots n} \end{pmatrix}$,

$U_R = \left[(U_R)_0 \cdots (U_R)_i \cdots (U_R)_{ij} \cdots (U_R)_{1\cdots n}\right]^T$, then

$U = \begin{pmatrix} (U_R)_0 - \sum_{1\leqslant i\leqslant n} (U_R)_i e_i - \sum_{1\leqslant i<j\leqslant n} (U_R)_{ij} e_{ij} \\ - \cdots - (U_R)_{1\cdots n} e_{1\cdots n} \end{pmatrix}$.

3) $V = \begin{pmatrix} E_0(V) + \sum_{1\leqslant i\leqslant n} E_i(V)e_i + \sum_{1\leqslant i<j\leqslant n} E_{ij}(V)e_{ij} \\ + \cdots + E_{1\cdots n}(V)e_{1\cdots n} \end{pmatrix}$,

$V_R = \left[(V_R)_0 \cdots (V_R)_i \cdots (V_R)_{ij} \cdots (V_R)_{1\cdots n}\right]^T$, then

$V = \begin{pmatrix} (V_R)_0 - \sum_{1\leqslant i\leqslant n} (V_R)_i e_i - \sum_{1\leqslant i<j\leqslant n} (V_R)_{ij} e_{ij} \\ - \cdots - (V_R)_{1\cdots n} e_{1\cdots n} \end{pmatrix}$. where $1 \leqslant i < j \leqslant n$, $row_{odd}^{2^{n-1}}(P)$ and $col_{odd}^{2^{n-1}}(P)$ denote the odd rows and odd columns extracted from matrix P for 2^{n-1} times respectively.

B. GA DICTIONARY TRAINING ANALYSIS

With the unknown variables, dictionary and coefficients, the dictionary training process using GA can be regarded as an extension of the sparse model put forward in (14), and can be formulated as

$$\{\hat{D}\,\hat{A}\} = argmin_{D,A} \|F - DA\|_F^2 + \gamma \|A\|_0 \quad (23)$$

where $F = \{f_i, 1 \leqslant i \leqslant K\} \in (\mathbb{G}_n)^{N\times K}$ is a series of the sample image patches, $D = \{d_i, 1 \leqslant i \leqslant M\} \in (\mathbb{G}_n)^{N\times M}$ is the GA dictionary with M atoms, $A = \{a_i, 1 \leqslant i \leqslant K\} \in (\mathbb{G}_n)^{M\times K}$ is the sparse coefficient matrix and $\|A\|_0$ counts the nonzero elements of the columns in A.

K-SVD [11] is a kind of fast and efficient sparse dictionary learning algorithm, whose key problem is how to learn sparse dictionary adaptively from the training data set, and it performs well for gray-scale image processing. However, when adapted to multispectral images, the main challenge is to capture the loss of relationship among different spectral channels during image reconstruction. In this paper, a dictionary training algorithm based on GA, called K-GASVD, is introduced as an extension of K-SVD [11] to cater to the multispectral images vectorization. Particularly, the GA-based dictionary training process contains two major steps, i.e., sparse coding stage and dictionary updating stage.

After extending to multispectral images processing, the orthogonal matching pursuit algorithm using GA (GAOMP) is designed to handle the sparse representation of GA multivector. The GAOMP algorithm deals with the problem of decomposing signal $F \in (\mathbb{G}_n)^{N\times K}$ on a GA dictionary $D \in (\mathbb{G}_n)^{N\times M}$ such that

$$A = argmin_A \|F - DA\|_2^2, \quad s.t.\ \|A\| \leqslant T \quad (24)$$

where $A \in (\mathbb{G}_n)^{M\times K}$ denotes the sparse coefficient vector and $\|A\| \leqslant T$ is the stopping criteria. Such operation helps to alleviate the problem of l_0-norm sparse coding that is usually seen as a NP-hard problem through assigning the maximum number of non-zero coefficients of each signal.

The details of GAOMP algorithm for each multispectral image patch are given in Table 1.

Once the sparse coding solution is obtained, the dictionary and sparse representation coefficient are updated simultaneously using GASVD. The details of K-GASVD algorithm is shown in Table 2:

C. FURTHER ANALYSIS

It is obvious that the introduced GAOMP algorithm in TABLE 1 is also a greedy algorithm, which mainly focuses

TABLE 1. The details of GA-based orthogonal matching pursuit algorithm.

Input: multispectral image patch: $f \in (\mathbb{G}_n)^N$; GA-based dictionary: $D = \{d_j, 1 \leqslant j \leqslant M\} \in (\mathbb{G}_n)^{N\times M}$; sparsity level: T.
Output: sparse coefficient: $a \in (\mathbb{G}_n)^M$.
1. Initialization: $i = 1, a^0 = 0, \varepsilon^0 = f - Da^0 = f, \Phi^0 = \varnothing$.
2. Set: $i = i + 1$.
3. Select j_0 $\forall j, s.t. min_k \left\|kd_{j_0} - \varepsilon^{i-1}\right\|_2 \leqslant min_k \left\|kd_j - \varepsilon^{i-1}\right\|_2$.
4. Set: $\Phi^i = \Phi^{i-1} \cup \{j_0\}$.
5. Calculate: $a^i = argmin_a \left\|Da - f\right\|_2, s.t. a = \Phi^i$.
6. Calculate: $\varepsilon^i = f - Da^i$.
7. When $i > T$, stop the iteration.

TABLE 2. The details of GA-based dictionary learning using K-GASVD method.

Input: multispectral image patches: $F = \{f_i, 1 \leqslant i \leqslant K\} \in (\mathbb{G}_n)^{N\times K}$; GA-based dictionary: $D = \{d_i, 1 \leqslant i \leqslant M\} \in (\mathbb{G}_n)^{N\times M}$; the number of iterations: J.
Output: sparse coefficient: $A = \{a_i, 1 \leqslant i \leqslant K\} \in (\mathbb{G}_n)^{M\times K}$; dictionary after training: $D \in (\mathbb{G}_n)^{N\times M}$.
1. Initialization: $j = 0$, initialize the GA-based dictionary $D \in (\mathbb{G}_n)^{N\times M}$ as random M samples from $F \in (\mathbb{G}_n)^{N\times K}$.
2. When $j < J$, repeat
(1) Sparse coding: compute sparse representation coefficient $a \in (\mathbb{G}_n)^M$ of $F \in (\mathbb{G}_n)^{N\times K}$ over $D \in (\mathbb{G}_n)^{N\times M}$ using GAOMP algorithm.
(2) Dictionary updating: update each dictionary atom $d_k \in (\mathbb{G}_n)^N$ in D^{J-1}.
(i) Define the set of patches using the k-th dictionary atom (i) $d_k \in (\mathbb{G}_n)^N$ as $\Omega_k = \{i \mid 1 \leqslant i \leqslant k, A(k,i) \neq 0\}$.
(ii) Calculate the sparse error matrix E_k without using d_k.
$E_k = F - \sum_{i\neq k} D_i a^i$
(iii) Select columns of E_k corresponding to Ω_k to form E_k^Ω.
$E_k^\Omega = E_k(:,i)|_{i=\Omega_k}$
(iv) Perform the SVD of E_k^Ω using GASVD: $E_k^\Omega = U\Sigma V^H$ and update d_k as $U(:,1)$, set $a_\Omega^k = \Omega_k^T a^k$ to be $V^H(:,1)\Sigma(1,1)$.

on selecting an atom that best matches the signal from the dictionary according to certain criteria during each iteration to sparsely approximate the original signal. Similar to the traditional OMP algorithm for scalar data [36], the introduced GAOMP algorithm is designed for multidimensional signals, typically for multispectral images, based on GA. At each step, the best atom which denotes the maximum of its inner product with the residual, is selected from GA dictionary, and then the residual is updated by conducting an orthogonal projection of the signal approximated onto the vectorial space which is generated by the chosen atoms formerly. Clearly, this orthogonalization shows its absolute importance since it makes the convergence of this greedy algorithm more stably and faster.

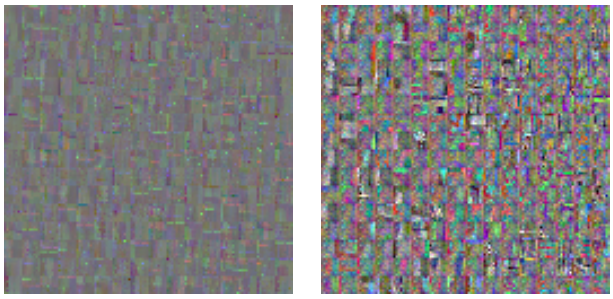

(a) (b)

FIGURE 1. Visualization of the color image dictionaries learned by K-SVD (a) and K-GASVD (b) methods.

For the introduced GAOMP algorithm, because of the introduction of GA, the result of inner product includes all the components of multispectral images, rather than a single component of original grayscale image. Therefore, during the iterations, the sparsity of all the spectral channels rather than a single channel is always guaranteed. So, all the components of multispectral images are processed integrally and monolithically while searching for the nearest atom.

Moreover, the convergence of the provided K-GASVD is similar to that of K-SVD, since it applies the same framework as the traditional K-SVD [9], [11], [13]. Fig. 1 shows the trained dictionaries based on K-SVD and K-GASVD methods. We observe that the learned dictionary using K-SVD method shows high tendency to be monochromatic. Since the K-SVD algorithm cannot perfectly handle the rich spectral components of the original multispectral images, which produces a large number of grayscale blocks in the training dictionary, resulting in some unsatisfying results of the reconstructed image, such as color is not rich enough and the color saturation is significantly reduced. In contrast, the learned dictionary based on K-GASVD method captures more color information since both the relationship of spectral channels and the spatial coherence are retained better.

$$F_R = \begin{bmatrix} E_0(F) & \cdots & E_t(F) & \cdots & -E_{ts}(F) & \cdots & (-1)^{n(n-1)/2}E_{1\cdots n}(F) \\ \vdots & \vdots & \vdots & \vdots & \vdots & \vdots & \vdots \\ E_t(F) & \cdots & E_0(F) & \cdots & -E_s(F) & \cdots & (-1)^{(t-1)+(n(n-1)/2)}E_{1\cdots n}(F) \\ \vdots & \vdots & \vdots & \vdots & \vdots & \vdots & \vdots \\ E_{ts}(F) & \cdots & -E_s(F) & \cdots & E_0(F) & \cdots & (-1)^{(t-1)+(s-2)+(n(n-1)/2)}E_x(F) \\ \vdots & \vdots & \vdots & \vdots & \vdots & \vdots & \vdots \\ E_{1\cdots n}(F) & \cdots & (-1)^{(n-t)}E_y(F) & \cdots & (-1)^{(2n-t-s+1)}E_x(F) & \cdots & E_0(F) \end{bmatrix}$$

$$\text{where } x = 1\cdots(t-1)(t+1)\cdots(s-1)(s+1)\cdots n;\ y = 1\cdots(t-1)(t+1)\cdots n;$$
$$t = 1\cdots n;\ i \neq t, t \neq s, j \neq t, j \neq s; j > i, s > t;\ E_{ij} = E_{ji} \quad \text{and} \quad F_R \in \mathbb{R}^{2^n M\times 2^n N}. \tag{22}$$

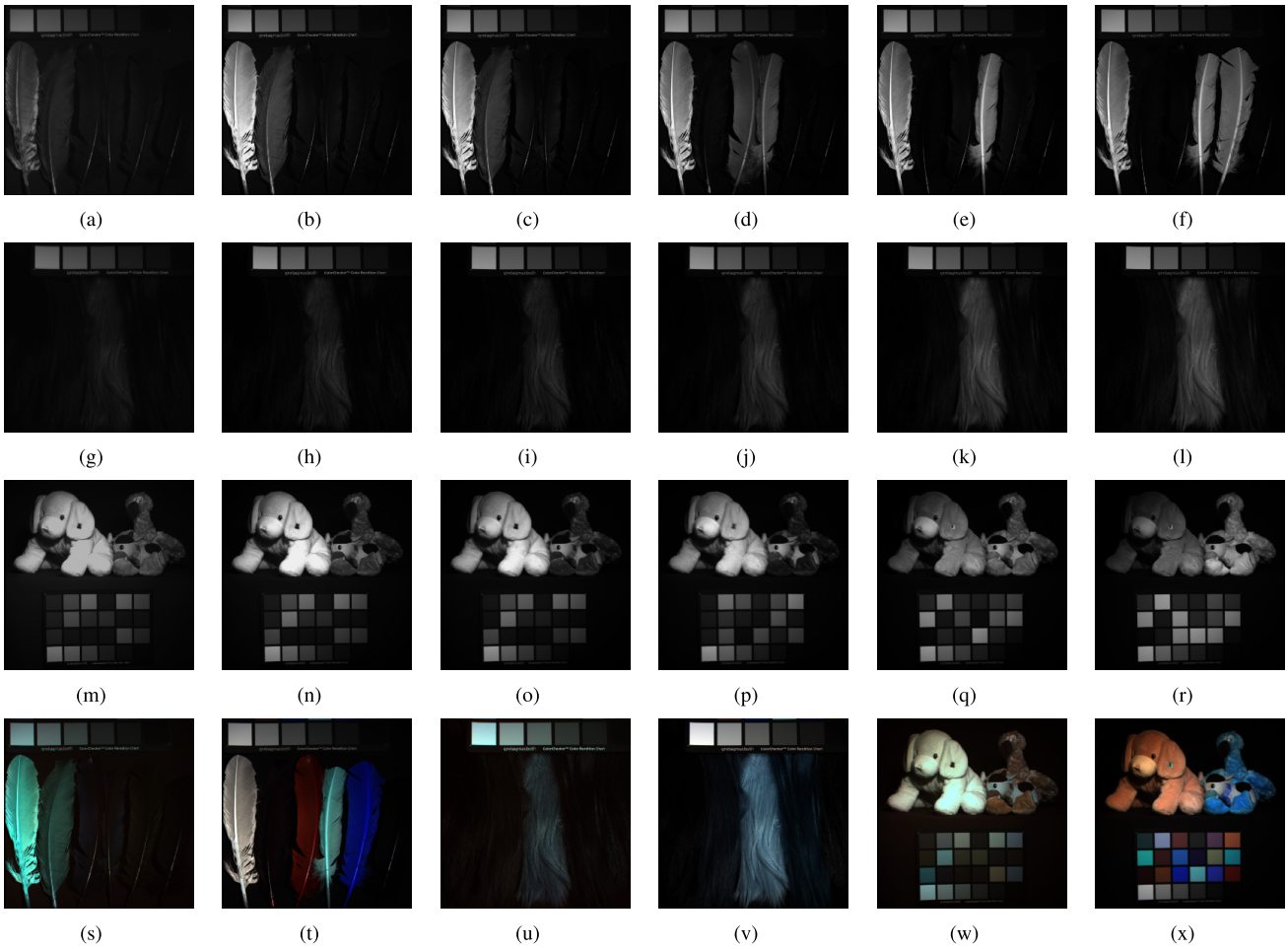

FIGURE 2. Examples of multispectral images. (a), (g), (m) band 2 images; (b), (h), (n) band 5 images; (c), (i), (o) band 7 images; (d), (j), (p) band 12 images; (e), (k), (q) band 20 images; (f), (l), (r) band 25 images; (s), (u), (w) the pseudo color images using 2, 5, and 7 band images as the RGB input; (t), (v), (x) the pseudo color images using 12, 20, and 25 band images as the RGB input.

V. EXPERIMENTAL ANALYSIS

To demonstrate the effectiveness and powerfulness of the proposed multivector sparse representation model for multispectral image processing, we perform both reconstruction and denoising experiments on both Columbia Multispectral Image Database [37] and Hyperspectral Image Database of Real-world Scenes [38] and compare the experimental results both quantitatively and visually.

A. DATA SETS

1) MULTISPECTRAL IMAGE DATASETS

The Columbia Multispectral Image Database [37] is utilized in our experiments. In this multispectral image data set, there are 32 real-world scenes consisting of various real objects and materials, each with spectral resolution 31 and spatial resolution 512 $\times$ 512, which includes full spectral resolution reflectance data collected from 400nm to 700nm in 10nm steps. More details can be found in http://www.cs.columbia.edu/CAVE/databases/multispectral/.

In our experiments, several arbitrary multispectral images are selected from the data set above to evaluate the performance of our K-GASVD method. Due to the limitation of the existing sparse models which can only deal with an ordinary gray-scale image or color image, we randomly select 6 bands from the chosen multispectral images to form 20 pseudo color images, respectively. Fig. 2(a)-(f), (g)-(l) and (m)-(r) show the images of band 2, 5, 7, 12, 20 and 25 belong to three multispectral images, respectively. Fig. 2(s)-(t), (u)-(v) and (w)-(x) show the two pseudo color images in which band 2, 5, and 7 images and are 12, 20, and 25 images input as the R, G and B channels, respectively.

2) HYPERSPECTRAL IMAGE DATASETS

Since hyperspectral images include per-pixel irradiance measurements in a number of narrow bands of wavelength in the visible spectrum, they provide higher spectral resolution and more spectral channels than multispectral images. Therefore, Hyperspectral Image Database of Real-world Scenes [38] is involved in this paper to further validate the advantages and good performance of the proposed sparse representation model. Hyperspectral Image Database of Real-world Scenes collected fifty images under daylight illumination, both outdoors and indoors, using a commercial hyperspectral camera

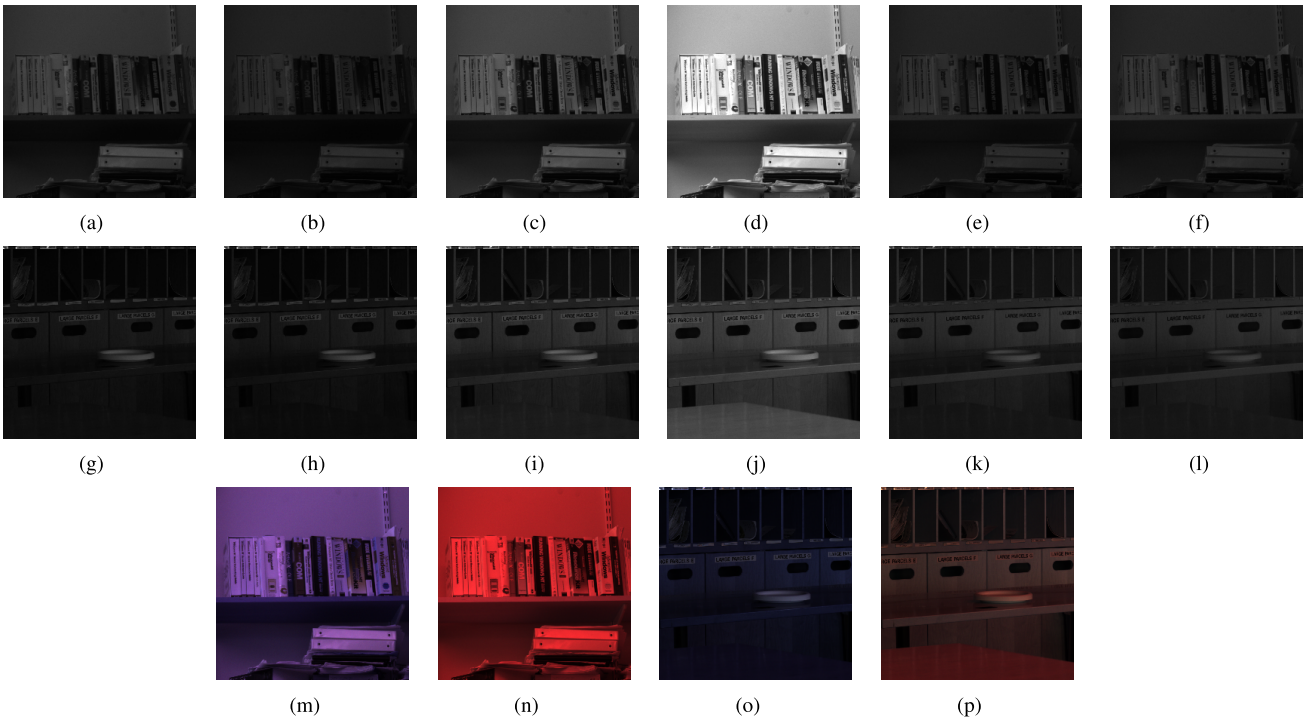

FIGURE 3. Examples of hyperspectral images. (a) and (g) band 8 images; (b) and (h) band 9 images; (c) and (i) band 15 images; (d) and (j) band 19 images; (e) and (k) band 25 images; (f) and (l) band 30 images; (m) and (o) the pseudo color images using 8, 9, and 15 band images as the RGB input; (n) and (p) the pseudo color images using 15, 19, and 30 band images as the RGB input.

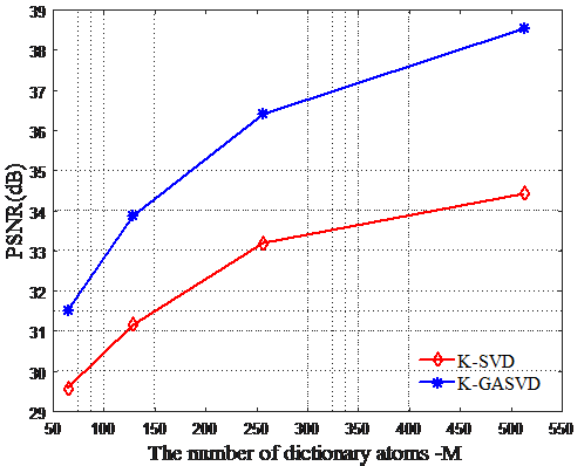

FIGURE 4. Comparison of K-GASVD and K-SVD based sparse models for multispectral images reconstruction-PSNR values vs. the number of dictionary atoms M.

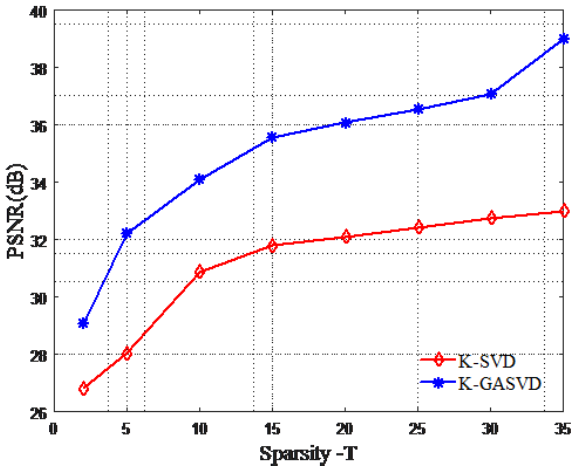

FIGURE 5. Comparison of K-GASVD and K-SVD sparse models for multispectral images reconstruction-PSNR values vs. sparse parameter T.

(Nuance FX, CRI Inc.) The camera uses an integrated liquid crystal tunable filter and is capable of acquiring a hyperspectral image by sequentially tuning the filter through a series of thirty-one narrow wavelength bands, each with approximately 10nm bandwidth and centered at steps of 10nm from 420nm to 720nm.

In our experiments, we arbitrarily select several hyperspectral images from the data set above to evaluate the performance of the proposed K-GASVD method. Fig. 3 shows two hyperspectral images with 6 spectral bands (band 8, 9, 15, 19, 25 and 30) respectively, and some pseudo color images formed by those bands.

B. MULTISPECTRAL IMAGES RECONSTRUCTION

As described above, the K-SVD based model [11] has achieved excellent results for gray-scale images processing, but for multispectral images, it just applies K-SVD method independently onto each spectral channel, leading to unsatisfying reconstruction results.

Therefore, in this section, we mainly prove the reconstruction results of the proposed K-GASVD based sparse

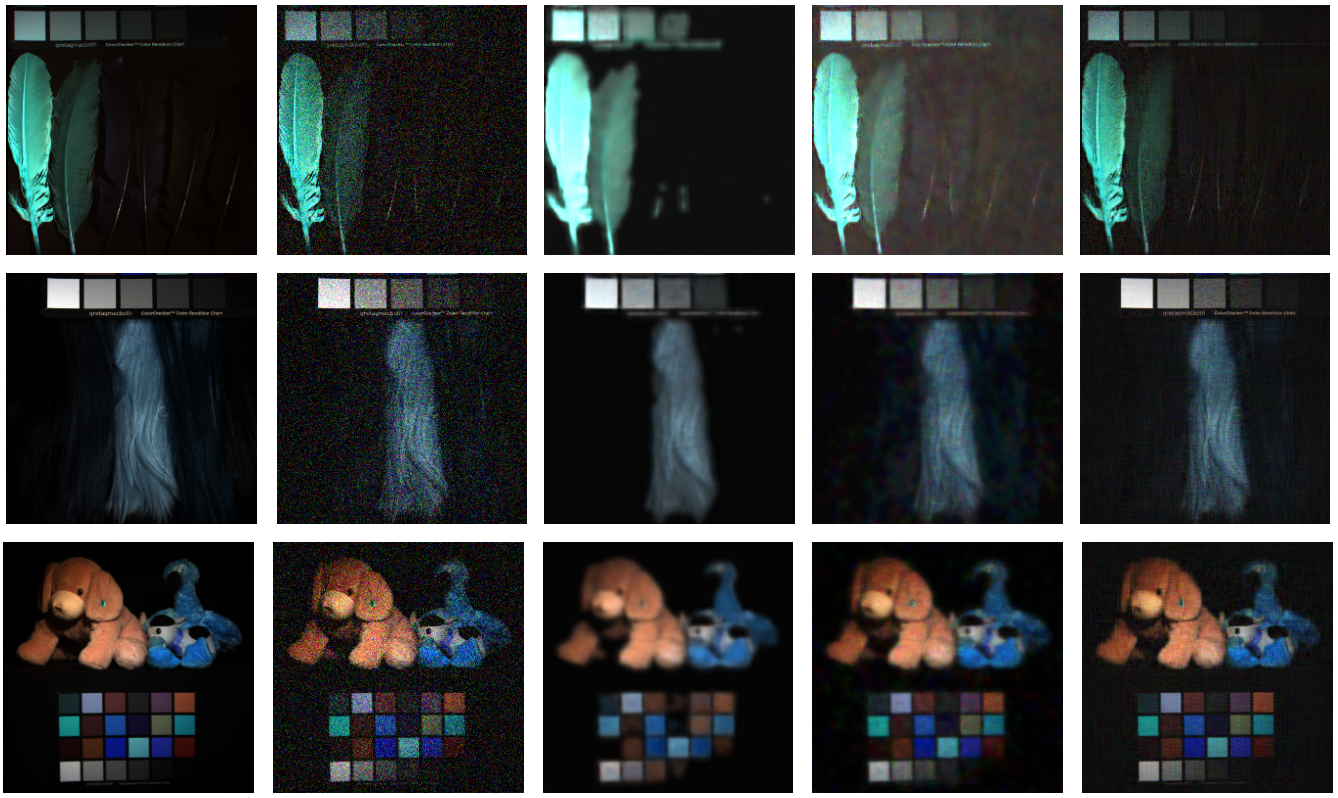

FIGURE 6. Denoising results of multispectral images. (a) Original Images, (b) Noisy Images ($\delta = 30$), (c) K-SVD [11], (d) improved K-SVD [16], (e) K-GASVD.

model experimentally, and compare it with the results of K-SVD based model under the same parameter condition. Considering reasonable computational complexity and the fairness of comparison, we set the size of multispectral image patches to 8×8.

As shown in Fig. 4, the proposed K-GASVD based sparse model significantly improves the reconstruction performance and the improvement becomes even more remarkable with respect to the increasing number of selected atoms. We further compare the number of atoms used of the two sparse models under the same PSNR. For example, it is clearly that, when the PSNR value get to nearly 34, the numbers of atoms corresponding to the K-SVD and K-GASVD models are about 450 and 150 respectively. That is to say, only approximate 1/3 number of atoms are needed in the K-GASVD model than that in K-SVD model [11] for similar reconstruction performance achievement with a reasonable sparse parameter. Clearly, the GA-based dictionary shows its capability in more colorful structures presentation, which manifests lower intra-redundancy of spectral channels of each atom in the multispectral images. Moreover, while using more dictionary, the proposed K-GASVD model reveals great performance more obviously.

Then, the influence of sparse parameter is considered for both models by computing the PSNR (dB) values under different sparse parameter T, and the results are shown as two curves in Fig.5.

It can be clearly seen from Fig. 5 that with the increasing number of sparse parameter T, the growth trends of the two curves are basically the same. Moreover, under the same sparse parameter T, the proposed K-GASVD model can obtain much higher PSNR values compared to the K-SVD model [11].

C. MULTISPECTRAL IMAGE DENOISING

Then, another application for multispectral images-denoising experiments are conducted on various multispectral images at different noise levels. First, let F_0 be a clean multispectral image represented in the GA form, denoted as a column vector of length N. Then the noisy version is

$$Y = F_0 + w \tag{25}$$

where $F_0 = \left\{f_{0i} \in (\mathbb{G}_n)^N, 1 \leqslant i \leqslant K\right\} \in (\mathbb{G}_n)^{N\times K}$ and w is a white Gaussian noise in the GA form (zero means and deviation δ). Then we consider the image patches of size $\sqrt{N} \times \sqrt{N}$, which are overlapping extracted from the noisy multispectral images, ordered as column vectors $y \in (\mathbb{G}_n)^N$, and $Y = \{y_i, 1 \leqslant i \leqslant K\} \in (\mathbb{G}_n)^{N\times K}$. Handling the multispectral images denoising problem using a sparse decomposition technique per overlapped patch is then converted to

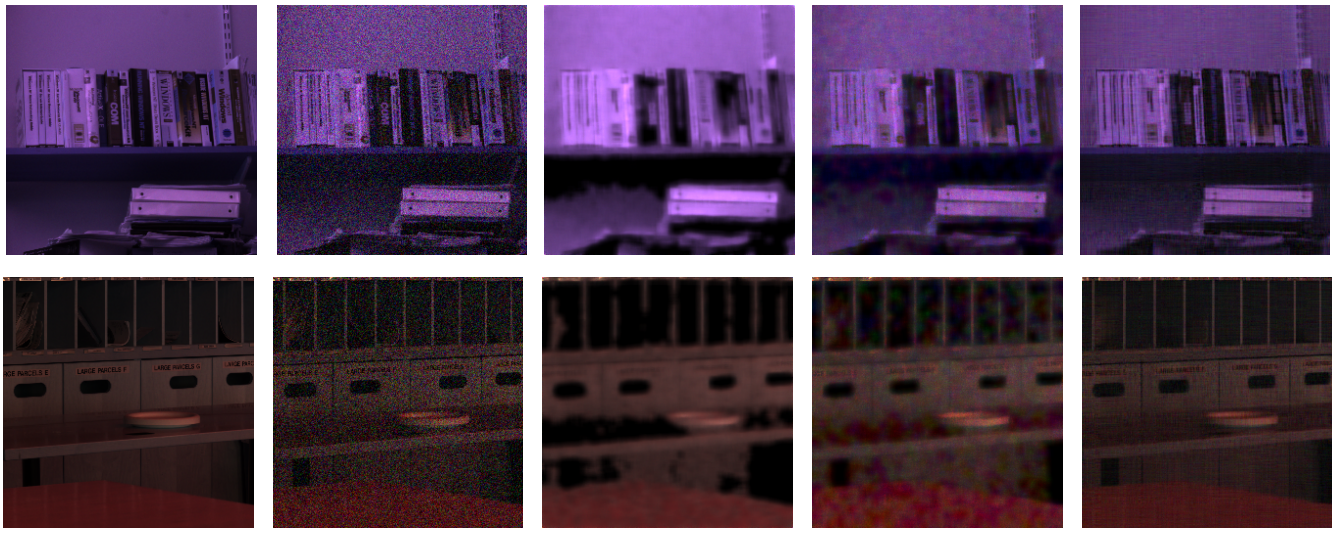

FIGURE 7. Denoising results of hyperspectral images. (a) Original Images, (b) Noisy Images ($\delta = 30$), (c) K-SVD [11], (d) improved K-SVD [16], (e) K-GASVD.

TABLE 3. PSNR values (dB) obtained by different denoising methods at each noisy level based on multispectral image datasets[37].

δ	methods	balloon	pepper	feather	superball	flower	bead
15	K-SVD[11]	36.61	35.77	35.39	36.27	36.66	35.22
	improved K-SVD[16]	36.89	36.08	36.42	36.90	37.01	36.05
	K-GASVD	39.51	37.37	38.69	38.49	39.38	38.32
20	K-SVD[11]	34.31	34.42	32.62	34.51	34.94	33.17
	improved K-SVD[16]	34.89	34.67	32.98	35.01	35.32	34.03
	K-GASVD	38.70	36.07	37.11	37.33	37.71	36.71
25	K-SVD[11]	32.60	31.63	31.34	30.82	31.36	31.09
	improved K-SVD[16]	32.93	31.95	32.02	31.23	31.94	31.64
	K-GASVD	34.57	32.35	33.29	33.00	35.45	34.43
30	K-SVD[11]	29.88	28.59	28.58	28.51	29.25	28.87
	improved K-SVD[16]	29.92	28.89	28.87	28.82	29.67	29.34
	K-GASVD	30.96	30.05	30.55	30.28	30.65	30.56

solve the following minimization problem:

$$\left\{\hat{D}, \hat{a}_{kl}, \hat{F}\right\} = min_{\hat{D},\hat{a}_{kl},\hat{F}_0} \gamma \|Y - F\|_2^2 + \sum_{k,l} \eta_{kl} \|a_{kl}\|_0 + \sum_{k,l} \|Da_{kl} - J_{kl}Y\|_2^2 \quad (26)$$

where $\hat{F}$ and the GA dictionary $\hat{D} \in (\mathbb{G}_n)^{N\times M}$ with M atoms denote estimators of F_0 and the optimal dictionary, respectively. Here, the optimal dictionary makes representation of recovered image patches to be sparsest. The indices $[k, l]$ indicates the location of the patch in the image. The vectors $\hat{a}_{kl}$ are the sparse representations for the $[k, l]$ -th patch in $\hat{F}$ using the dictionary $\hat{D}$. The operator J_{kl} extracts the patch of coordinates $[k, l]$ from the image.

Clearly, the first term in (26) indicates the probability that requires a proximity between $\hat{F}$ and Y. The image prior are exactly posed by both the second and the third terms, in which the sparsest representation and the consistency of the decomposition are provided and ensured by the second and third terms respectively. This regularization term provides an assumption that good-characterized natural images are to exhibit the sparse representation for every patch in the image over the learned dictionary $\hat{D}$.

Considering reasonable computational complexity and the fairness of comparison, we set, the number of iterations $J = 30$, the size of multispectral image patches to 8×8 and the number of both dictionary atoms $M = 256$.

Firstly, we validate the results achieved by applying the monochromatic model based on K-SVD method [11], the concatenation model based on improved K-SVD method [16] and our multivector model based on K-GASVD method, on the testing multispectral images shown in Fig.2 and hyperspectral images shown in Fig.3 with the noise deviation $\delta = 30$, in order to enable a fair comparison. Fig. 6 and Fig. 7 show the comparison of the K-SVD, the improved K-SVD and our proposed K-GASVD models in terms of denoising results. Notice that, for the multispectral and hyperspectral images, there is no existing sparse model, the general method is to regard each single-band image of the multispectral or hyperspectral image as a gray-scale image to process them respectively, such as the

TABLE 4. SSIM values obtained by different denoising methods at each noisy level based on hyperspectral image datasets[38].

δ	methods	img3	img4	imgd0	imgd5	imgg8	imgg9
15	K-SVD[11]	0.8738	0.8743	0.8404	0.8621	0.8878	0.8326
	improved K-SVD[16]	0.8757	0.8862	0.8496	0.8636	0.8941	0.8902
	K-GASVD	0.9051	0.9073	0.8869	0.8949	0.9105	0.9102
20	K-SVD[11]	0.8628	0.8649	0.8343	0.8532	0.8419	0.7859
	improved K-SVD[16]	0.8662	0.8670	0.8394	0.8546	0.8560	0.8397
	K-GASVD	0.8938	0.8967	0.8671	0.8833	0.8913	0.8697
25	K-SVD[11]	0.8261	0.8249	0.7809	0.8202	0.7868	0.7529
	improved K-SVD[16]	0.8301	0.8306	0.7775	0.8242	0.8199	0.7889
	K-GASVD	0.8657	0.8715	0.8827	0.8504	0.8370	0.8689
30	K-SVD[11]	0.7977	0.7918	0.7268	0.7949	0.7365	0.7239
	improved K-SVD[16]	0.8020	0.7989	0.7315	0.7979	0.7952	0.7408
	K-GASVD	0.8566	0.8605	0.8585	0.8382	0.8229	0.8408

K-SVD method, or concatenate all the spectral channels into a single vector using a shared sparse coefficient, such as the improved K-SVD method. As shown in Fig. 6 and Fig. 7, the K-SVD based model is performed in a monochromatic way, which ignores the correlation among these spectral channels and loses the inherent spectral structures, which introduces a hue bias and leads to a lack of details. The improved K-SVD based sparse model reduces some hue bias, but still loses channel interrelationship and produces some false colors and artifacts.

In the high-frequency texture areas, our K-GASVD sparse model that regards a multispectral or hyperspectral image as a GA multivector, has a clear advantage over the K-SVD and the improved K-SVD methods that either represent each single-band image as a scalar or concatenate all the spectral channels into a single channel.

We now turn to study the influence of different noise levels. To evaluate the superiority of our K-GASVD method objectively, the denoising results represented by PSNR and SSIM, which are achieved by applying our proposed method,

$$
\begin{aligned}
f &= Da \Leftrightarrow 0 + \sum_{1\leqslant i\leqslant n} E_i(f)e_i + \sum_{1\leqslant i<j\leqslant n} E_{ij}(f)e_{ij} + \cdots + E_{1\cdots n}(f)e_{1\cdots n} \\
&= \left(E_0(D)E_0(a) + \sum_{1\leqslant i\leqslant n} E_i(D)E_i(a) - \sum_{1\leqslant i<j\leqslant n} E_{ij}(D)E_{ij}(a) + \cdots + (-1)^{n(n-1)/2}E_{1\cdots n}(D)E_{1\cdots n}(a) \right) e_0 \\
&\quad + \cdots + \begin{pmatrix} E_t(D)E_0(a) + \frac{i-t}{|i-t|}\sum_{1\leqslant i\leqslant n} E_{ti}(D)E_i(a) \\ +E_0(D)E_t(a) + \frac{t-i}{|t-i|}\sum_{1\leqslant i\leqslant n} E_i(D)E_{it}(a) \\ [3pt] + \cdots + (-1)^{(t-1)+(n(n-1)/2)}E_{1\cdots(t-1)(t+1)\cdots n}(D)E_{1\cdots n}(a) \end{pmatrix} e_t \\
&\quad + \cdots + \begin{pmatrix} E_{ts}(D)E_0(a) + \frac{(i-t)(i-s)}{|i-t||i-s|}\sum_{1\leqslant i\leqslant n} E_{tsi}(D)E_i(a) + E_t(D)E_s(a) - E_s(D)E_t(a) \\ +\frac{(i-t)(i-s)(j-t)(j-s)}{|i-t||i-s||j-s||j-t|}\sum_{1\leqslant i<j\leqslant n} E_{tsij}(D)E_{js}(a) + \frac{(j-t)(s-j)}{|j-t||s-j|}\sum_{1\leqslant j\leqslant n} E_{tj}(D)E_{js}(a) \\ + \cdots + (-1)^{(t-1)+(s-2)+(n(n-1)/2)}E_{1\cdots(t-1)(t+1)\cdots(s-1)(s+1)\cdots n}(D)E_{1\cdots n}(a) \end{pmatrix} e_{ts} \\
&\quad + \cdots + \begin{pmatrix} E_{1\cdots n}(D)E_0(a) + (-1)^{(n-i)}\sum_{1\leqslant i\leqslant n} E_{1\cdots(i-1)(i+1)\cdots n}(D)E_i(a) \\ +(-1)^{(2n-i-j+1)}\sum_{1\leqslant i<j\leqslant n} E_{1\cdots(i-1)(i+1)\cdots(j-1)(j+1)\cdots n}(D)E_{ij}(a) + E_0(D)E_{1\cdots n}(a) \end{pmatrix} e_{1\cdots n} \\
&\textit{where } e_0 = 1; t = 1, \cdots, n; i \neq t, i \neq s, j \neq t, j \neq s; j > i, s > t; E(D)_{ij} = E(D)_{ji}; E(Da)_{ij} = E(Da)_{ji}. \qquad (28)
\end{aligned}
$$

$$
\tilde{a} = \begin{bmatrix}
E_0(a) & \cdots & E_t(a) & \cdots & -E_{ts}(a) & \cdots & (-1)^{n(n-1)/2}E_{1\cdots n}(a) \\
\vdots & \vdots & \vdots & \vdots & \vdots & \vdots & \vdots \\
E_t(a) & \cdots & E_0(a) & \cdots & -E_s(a) & \cdots & (-1)^{(t-1)+(n(n-1)/2)}E_{1\cdots n}(a) \\
\vdots & \vdots & \vdots & \vdots & \vdots & \vdots & \vdots \\
E_{ts}(a) & \cdots & -E_s(a) & \cdots & E_0(a) & \cdots & (-1)^{(t-1)+(s-2)+(n(n-1)/2)}E_x(a) \\
\vdots & \vdots & \vdots & \vdots & \vdots & \vdots & \vdots \\
E_{1\cdots n}(a) & \cdots & (-1)^{(n-t)}E_y(a) & \cdots & (-1)^{(2n-t-s+1)}E_x(a) & \cdots & E_0(a)
\end{bmatrix}
$$

$$
\begin{aligned}
&\textit{where } x = 1\cdots(t-1)(t+1)\cdots(s-1)(s+1)\cdots n; y = 1\cdots(t-1)(t+1)\cdots n; t = 1\cdots n; \\
&i \neq t, t \neq s, j \neq t, j \neq s; j > i, s > t; E_{ij} = E_{ji}. \qquad (29)
\end{aligned}
$$

the improved K-SVD method and the K-SVD method over several noise levels on the same testing multispectral and hyperspectral images are collected in Table 3 and 4. The noise deviation δ are set to be 15, 20, 25 and 30. It is shown in Table 3 and 4, the improved K-SVD method shows better denoising results compared to the K-SVD method, for it partly reserves the inherent spectral structure with the use of concatenated channel. However, it still produces some hue bias and artifacts. Our proposed method outperforms the results of the K-SVD and the improved K-SVD methods, better results are achieved with small values of δ and vice versa. In fact, this is expected because relatively ''clean'' images have a greater impact on the outcome, on the contrary, very noisy images have a weak influence on the results, if any. It is mainly because our proposed K-GASVD method attains the inherent spectral structure of multispectral images to reserve more details and avoid the artifacts.

VI. CONCLUSION

This work has put forward a new sparse representation model based on geometric algebra (GA) for multispectral images processing, resulting in state-of-the-art performance and exceeding recent leading alternatives. The proposed sparse model treats a multispectral image as a GA multivector, totally preserves the relationships of the spectral channels to avoid the loss of inherent spectral structures. Besides, we provide a GA-based dictionary learning method, called K-GASVD method, which can capture the important spectral space-related information while capturing the important spectral structure information, and replace the sparse dictionary of several channels with a GA dictionary. The reconstruction and denoising experiments demonstrate the superiority of the proposed model and show its potential in multispectral images processing and analysis.

APPENDIX

A. DERIVATION OF THE GENERALIZED FORM OF SPARSE REPRESENTATION MODEL BASED ON GA

Then, the generalized form of representation model for multispectral images can be obtained as follows

$$\begin{aligned}&\left[0 \ \cdots \ E_i(f) \ \cdots \ E_{ij}(f) \ \cdots \ E_{1\cdots n}(f)\right]\\&= \left[E_0(D) \ \cdots \ E_i(D) \ \cdots \ E_{ij}(D) \ \cdots \ E_{1\cdots n}(D)\right]\tilde{a} \quad (27)\end{aligned}$$

According to the relationship of a multispectral image $F \in (\mathbb{G}_n)^{N\times K}$, the GA dictionary $D \in (\mathbb{G}_n)^{N\times M}$ and the sparse coefficient vector $a \in (\mathbb{G}_n)^M$ shown in (28), shown at the bottom of the previous page.

Therefore, we can obtain the generalized sparse coefficient matrix $\tilde{a} \in \mathbb{R}^{2^n M\times 2^n N}$ shown in (29), as shown at the bottom of the previous page.

REFERENCES

[1] A. B. Said, R. Hadjidj, K. E. Melkemi, and S. Foufou, ''Multispectral image denoising with optimized vector non-local mean filter,'' *Digit. Signal Process.*, vol. 58, pp. 115–126, Nov. 2016.
[2] S. Tzoumas, A. Rosenthal, C. Lutzweiler, D. Razansky, and V. Ntziachristos, ''Spatiospectral denoising framework for multispectral optoacoustic imaging based on sparse signal representation,'' *Med. Phys.*, vol. 41, no. 11, p. 113301, 2014.
[3] Q. Xie *et al.*, ''Multispectral images denoising by intrinsic tensor sparsity regularization,'' in *Proc. Comput. Vis. Pattern Recognit.*, Jun. 2016, pp. 1692–1700.
[4] D. Valsesia and E. Magli, ''A novel rate control algorithm for onboard predictive coding of multispectral and hyperspectral images,'' *IEEE Trans. Geosci. Remote Sens.*, vol. 52, no. 10, pp. 6341–6355, Oct. 2014.
[5] P. Valsesia, S. Jeyakumar, and N. Nithiyanandam, ''Hyper spectral image compression based on non-iterative matrix factorization,'' in *Proc. IEEE Int. Conf. Comput. Intell. Comput. Res. (ICCIC)*, Dec. 2013, pp. 1–4.
[6] R. Kawakami, Y. Matsushita, J. Wright, M. Ben-Ezra, Y.-W. Tai, and K. Ikeuchi, ''High-resolution hyperspectral imaging via matrix factorization,'' in *Proc. Comput. Vis. Pattern Recognit.*, vol. 42, Jul. 2011, pp. 2329–2336.
[7] A. Chen, ''The inpainting of hyperspectral images: A survey and adaptation to hyperspectral data,'' *Proc. SPIE*, vol. 8537, pp. 85371K-1–85371K-8, Nov. 2011.
[8] H. van Nguyen, A. Banerjee, and R. Chellappa, ''Tracking via object reflectance using a hyperspectral video camera,'' in *Proc. IEEE Comput. Soc. Conf. Comput. Vis. Pattern Recognit. Workshops*, Jun. 2011, pp. 44–51.
[9] M. Aharon, M. Elad, and A. M. Bruckstein, ''K-SVD: An algorithm for designing overcomplete dictionaries for sparse representation,'' *IEEE Trans. Image Process.*, vol. 54, no. 11, pp. 4311–4322, Nov. 2006.
[10] J. Wright, Y. Ma, J. Mairal, G. Sapiro, T. S. Huang, and S. Yan, ''Sparse representation for computer vision and pattern recognition,'' *Proc. IEEE*, vol. 98, no. 6, pp. 1031–1044, Jun. 2010.
[11] M. Elad and M. Aharon, ''Image denoising via sparse and redundant representations over learned dictionaries,'' *IEEE Trans. Image Process.*, vol. 15, no. 12, pp. 68–80, Dec. 2006.
[12] O. G. Guleryuz, ''Nonlinear approximation based image recovery using adaptive sparse reconstructions and iterated denoising—Part I: Theory,'' *IEEE Trans. Image Process.*, vol. 15, no. 3, pp. 539–554, Mar. 2006.
[13] Z. C. Wang, R. J. Jiang, X. Jiang, and T. Zhou, ''Learning sparse representations by K-SVD for facial expression classification,'' in *Proc. 4th Int. Conf. Comput. Sci. Netw. Technol. (ICCSNT)*, Dec. 2015, pp. 772–775.
[14] F. Chen, H. Yu, and R. Hu, ''Shape sparse representation for joint object classification and segmentation,'' *IEEE Trans. Image Process.*, vol. 22, no. 3, pp. 992–1004, Mar. 2013.
[15] S. Agarwal and D. Roth, ''Learning a sparse representation for object detection,'' in *Proc. Eur. Conf. Comput. Vis. (ECCV)*, 2006, pp. 97–101.
[16] J. Mairal, M. Elad, and G. Sapiro, ''Sparse representation for color image restoration,'' *IEEE Trans. Image Process.*, vol. 17, no. 1, pp. 53–69, Jan. 2008.
[17] L. Yu, Y. Xu, H. Xu, and H. Zhang, ''Quaternion-based sparse representation of color image,'' in *Proc. IEEE Int. Conf. Multimedia Expo (ICME)*, Jul. 2013, pp. 1–7.
[18] Y. Xu, L. Yu, H. Xu, H. Zhang, and T. Nguyen, ''Vector sparse representation of color image using quaternion matrix analysis,'' *IEEE Trans. Image Process.*, vol. 24, no. 4, pp. 1315–1329, Apr. 2015.
[19] R. Wang, Y. Wu, M. M. Shen, and W. Cao, ''Sparse representation for color image based on geometric algebra,'' in *Proc. IEEE Int. Conf. Multimedia Expo (ICME)*, Jul. 2018, pp. 1–6.
[20] M. Shen, R. Wang, and W. Cao, ''Joint sparse representation model for multi-channel image based on reduced geometric algebra,'' *IEEE Access*, vol. 6, pp. 24213–24223, 2018, doi: 10.1109/ACCESS.2018.2819691.
[21] M. Shen and R. Wang, ''A new singular value decomposition algorithm for octonion signal,'' in *Proc. 24th Int. Conf. Pattern Recognit. (ICPR)*, Aug. 2018, pp. 3233–3237.
[22] Q. Barthélemy, A. Larue, and J. I. Mars, ''Color sparse representations for image processing: Review, models, and prospects,'' *IEEE Trans. Image Process.*, vol. 24, no. 11, pp. 3978–3989, Nov. 2015.
[23] S. Franchini, A. Gentile, F. Sorbello, G. Vassallo, and S. Vitabile, ''ConformalALU: A conformal geometric algebra coprocessor for medical image processing,'' *IEEE Trans. Comput.*, vol. 64, no. 4, pp. 955–970, Apr. 2015.
[24] H. Su and Z. Bo, ''Conformal geometric algebra based band selection and classification for hyperspectral imagery,'' in *Proc. 8th Workshop Hyperspectral Image Signal Process., Evol. Remote Sens. (WHISPERS)*, Los Angeles, CA, USA, Aug. 2016, pp. 1–4.

[25] M. T. Pham, T. Yoshikawa, T. Furuhashi, and K. Tachibana, "Robust feature extractions from geometric data using geometric algebra," in *Proc. IEEE Int. Conf. Syst., Man, Cybern.*, Oct. 2009, pp. 529–533.
[26] J. Ebling and G. Scheuermann, "Clifford Fourier transform on vector fields," *IEEE Trans. Vis. Comput. Graphics*, vol. 11, no. 4, pp. 469–479, Jul. 2005.
[27] R. Wang, Y.-X. Zhou, Y.-L. Jin, and W.-M. Cao, "Sparse fast Clifford Fourier transform," *Frontiers Inf. Technol. Electron. Eng.*, vol. 18, no. 8, pp. 1131–1141, Aug. 2017.
[28] Y. Li, W. Liu, X. Li, Q. Huang, and X. Li, "GA-SIFT: A new scale invariant feature transform for multispectral image using geometric algebra," *Inf. Sci.*, vol. 281, pp. 559–572, Oct. 2014.
[29] B. Huang, H. Song, H. Cui, J. Peng, and Z. Xu, "Spatial and spectral image fusion using sparse matrix factorization," *IEEE Trans. Geosci. Remote Sens.*, vol. 52, no. 3, pp. 1693–1704, Mar. 2014.
[30] C. Lanaras, E. Baltsavias, and K. Schindler, "Advances in hyperspectral and multispectral image fusion and spectral unmixing," *Int. Arch. Photogramm. Remote Sens.*, vol. 40, no. 3, pp. 451–458, 2015.
[31] R. Dian, L. Fang, and S. Li, "Hyperspectral image super-resolution via non-local sparse tensor factorization," in *Proc. IEEE Conf. Comput. Vis. Pattern Recognit. (CVPR)*, Jul. 2017, pp. 3862–3871.
[32] K. Zhang, M. Wang, and S. Yang, "Spatial–spectral-graph-regularized low-rank tensor decomposition for multispectral and hyperspectral image fusion," *IEEE J. Sel. Topics Appl. Earth Observ. Remote Sens.*, vol. 11, no. 4, pp. 1030–1040, Apr. 2018.
[33] Y.-T. Shih, C.-S. Chien, and C.-Y. Chuang, "An adaptive parameterized block-based singular value decomposition for image de-noising and compression," *Appl. Math. Comput.*, vol. 218, no. 21, pp. 10370–10385, 2012.
[34] J. Huang, J. Xie, F. Li, and L. Li, "Compound de-noising method based on discrete stationary wavelet transform and optimized SVD," *Piezoelectr. Acoustoopt.*, vol. 35, no. 3, pp. 448–451, Jun. 2013.
[35] E.-L. Chen, X. Zhang, Y.-J. Shen, and X.-M. Cao, "Fault diagnosis of rolling bearings based on SVD denoising and blind signals separation," *J. Vib. Shock*, vol. 31, pp. 185–190, Dec. 2012.
[36] Y. C. Pati, "Orthogonal matching pursuit: Recursive function approximation with applications to wavelet decomposition," in *Proc. Asilomar Conf. Signals, Syst. Comput.*, Nov. 1993, pp. 40–44.
[37] F. Yasuma, T. Mitsunaga, D. Iso, and S. K. Nayar, "Generalized assorted pixel camera: Postcapture control of resolution, dynamic range, and spectrum," *IEEE Trans. Image Process.*, vol. 19, no. 9, pp. 2241–2253, Sep. 2010.
[38] A. Chakrabarti and T. Zickler, "Statistics of real-world hyperspectral images," in *Proc. IEEE Conf. Comput. Vis. Pattern Recognit. (CVPR)*, Jun. 2011, pp. 193–200.

RUI WANG received the B.S. and Ph.D. degrees in electronics and information engineering from Xidian University, Xi'an, Shaanxi, China, in 2004 and 2009, respectively. Since 2009, he has been with the School of Communication and Information Engineering, Shanghai University, where he is currently an Associate Professor. His research interests include sensor networks, geometric algebra, and multimedia signal processing.

MIAOMIAO SHEN received the B.S. degree in communication engineering from Shanghai University, Shanghai, China, in 2016, where she is currently pursuing the M.S. degree with the School of Communication and Information Engineering. She is currently committed to multimedia signal processing, the Internet of Things, and sparse representation mainly.

WENMING CAO received the Postdoctoral degree from Southeast University, Nanjing, China, in 2004, and the Ph.D. degree from the Institute of Automation, Beijing, in 2007. He is currently a Professor with the College of Information Engineering, Shenzhen University, Shenzhen, China, and a Visiting Professor with the Video Processing and Communication Laboratory, Department of Electrical and Computer Engineering, University of Missouri, Columbia, MO, USA. His research interests include signal processing and communication, media analysis and retrieval, and pattern recognition.